



1 **How will the key marine calcifier *Emiliana huxleyi* respond to a warmer and more**  
2 **thermally variable ocean?**

3

4

5 Xinwei Wang<sup>1</sup>, Feixue Fu<sup>2</sup>, Pingping Qu<sup>2</sup>, Joshua D. Kling<sup>2</sup>, Haibo Jiang<sup>3</sup>, Yahui Gao<sup>1,4</sup>,

6 David A. Hutchins<sup>2\*</sup>

7 1. School of Life Sciences, Xiamen University, Xiamen, 361005, China

8 2. Department of Biological Sciences, University of Southern California, Los Angeles,

9 California, 90089, USA

10 3. School of Life Sciences, Central China Normal University, Wuhan, Hubei, China.

11 4. Key Laboratory of the Ministry of Education for Coastal and Wetland Ecosystems,

12 Xiamen University, Xiamen 361005, China

13

14 \*Corresponding author: David Hutchins, tel: 1-213-7405616, fax: 1-213-7408123,

15 Email address: [dahutch@usc.edu](mailto:dahutch@usc.edu)

16

17 Key words: thermal variation, *Emiliana huxleyi*, coccolithophore, calcification, growth

18 rate, elemental composition, global warming

19

20



21 **Abstract**

22 Global warming will be combined with predicted increases in thermal variability in the  
23 future surface ocean, but how temperature dynamics will affect phytoplankton biology  
24 and biogeochemistry is largely unknown. Here, we examine the responses of the  
25 globally important marine coccolithophore *Emiliana huxleyi* to thermal variations at  
26 two frequencies (one-day and two-day) at low (18.5 °C) and high (25.5 °C) mean  
27 temperatures. Elevated temperature and thermal variation decreased growth,  
28 calcification and physiological rates, both individually and interactively. One-day  
29 thermal variation frequencies were less inhibitory than two-day variations under high  
30 temperature, indicating that high frequency thermal fluctuations may reduce heat-  
31 induced mortality and mitigate some impacts of extreme high temperature events.  
32 Cellular elemental composition and calcification was significantly affected by both  
33 thermal variation treatments relative to each other, and to the constant temperature  
34 controls. The negative effects of thermal variation on *E. huxleyi* growth rate and  
35 physiology are especially pronounced at high temperatures. These responses of the key  
36 marine calcifier *E. huxleyi* to warmer, more variable temperature regimes have  
37 potentially large implications for ocean productivity and marine biogeochemical cycles  
38 under a future changing climate.

39



40 **Introduction**

41 Climate-driven changes such as ocean warming alter the productivity and  
42 composition of marine phytoplankton communities, thereby influencing global  
43 biogeochemical cycles (Boyd et al., 2018; Hutchins & Fu, 2017; Thomas, et al., 2012).  
44 Increasing sea surface temperatures have been linked to global declines in  
45 phytoplankton concentration (Boyce, et al., 2010), changes in spring bloom timing  
46 (Friedland et al., 2018), and biogeographic shifts in harmful algal blooms (Gobler et al.,  
47 2017). Warming and acidification may drive shifts away from dinoflagellate or diatom  
48 dominance, and towards nanophytoplankton (Hare et al., 2007; Keys, et al., 2018).  
49 Similarly, Morán et al. (2010) predicted that a gradual shift will occur towards smaller  
50 primary producers in a warmer ocean.

51 Effects of temperature increases on phytoplankton diversity are uncertain.  
52 Warming and phytoplankton biodiversity were found to be inversely correlated in a  
53 coastal California diatom assemblage, at least on short timescales (Tatters et al., 2018).  
54 In contrast, a five-year long mesocosm experiment found that elevated temperature can  
55 modulate species coexistence, thus increasing phytoplankton species richness and  
56 productivity (Yvon-Durocher et al. 2015). Globally, rising temperatures may result in  
57 losses of phytoplankton biodiversity in the tropics, but gains in the polar regions  
58 (Thomas et al., 2012). It is thought that ocean warming will lead to a poleward range  
59 expansion of warm-water species at the expense of cold-water species (Boyd et al.,  
60 2010; Gao et al., 2018; Hallegraeff, 2010; Hutchins & Fu, 2017; Thomas et al., 2012).  
61 It is evident that rising ocean temperatures will benefit some groups, while having



62 detrimental consequences for others (Boyd et al., 2010, 2015, 2018; Feng, et al., 2017;  
63 Fu et al., 2014). For example, recent decades of satellite observations show a striking  
64 poleward shift in the distribution of blooms of the coccolithophore *Emiliana huxleyi*,  
65 a species that was previously virtually absent in polar waters (Boyd et al., 2010;  
66 Neukermans et al., 2018).

67 Coccolithophores are the most successful calcifying phytoplankton in the ocean,  
68 and contribute almost half of global marine calcium carbonate production. They play  
69 crucial biogeochemical roles by performing both photosynthesis and calcification, and  
70 facilitate carbon export to the deep ocean through the ballasting effects of their calcium  
71 carbonate shells (Klaas & Archer, 2002; Krumhardt et al., 2017; Monteiro et al., 2016).  
72 *E. huxleyi* (Lohm.) is the most abundant and cosmopolitan coccolithophore, forming  
73 prolific blooms in many regions (Holligan, et al., 1983; 1993; Iglesias-Rodríguez et al.,  
74 2002; Westbroek et al., 1993).

75 The responses of *E. huxleyi* to global change factors have been intensively  
76 investigated. Many *E. huxleyi* strains are sensitive to ocean acidification, which  
77 negatively affects their growth rates and calcification (Feng et al., 2018; Hoppe et al.,  
78 2011). However, among the many currently changing environmental drivers,  
79 temperature may be among the most important in regulating coccolithophore  
80 physiology (Boyd et al., 2010). Feng et al. (2008) reported that the growth rate of *E.*  
81 *huxleyi* was improved by elevated temperature at low irradiance. Furthermore,  
82 temperature was the most important driver controlling both cellular particulate organic  
83 and inorganic carbon content of a Southern Hemisphere *E. huxleyi* strain (Feng et al.,



84 2018).

85 Most research about the effects of global warming on *E. huxleyi* and  
86 phytoplankton in general has focused on predicted increases in mean temperatures.  
87 However, in the natural environment, seawater temperatures fluctuate over timescales  
88 ranging from hours, to days, to months (Bozinovic et al., 2011; Jiang et al., 2017).  
89 Future climate models predict not only an increase in mean temperature, but also an  
90 increase in temperature variability (frequency and intensity), as well as a higher  
91 probability of extreme events (IPCC 2014).

92 The impacts of climatic variability and extremes have been best studied in  
93 metazoans, where they may sometimes have a larger effect than increases in climatic  
94 averages alone (Vázquez et al., 2017; Vasseur et al., 2014; Zander et al., 2017).  
95 Variability can promote greater zooplankton species richness, compared with long-term  
96 average conditions (Cáceres 1997; Shurin et al. 2010). In corals, temperature variability  
97 could buffer warming stress, elevate thermal tolerance and reduce the risk of bleaching  
98 (Oliver & Palumbi, 2011; Safaie et al., 2018).

99 In comparison, we still lack a thorough understanding of how thermal variation  
100 affects phytoplankton growth and physiology. Unlike zooplankton, the few available  
101 studies suggest increasing thermal variation may decrease phytoplankton biomass and  
102 biodiversity, and shift the community towards small phytoplankton (Burgmer &  
103 Hillebrand, 2011; Rasconi et al., 2017). Two studies have shown that plastic responses  
104 play a key role in acclimation and adaptation to thermal fluctuations in algae (Kremer  
105 et al., 2018; Schaum & Collins, 2014). Population growth rates of phytoplankton in



106 fluctuating thermal environments have been quantitatively modeled based on data from  
107 thermal response curves obtained under constant temperatures (Bernhardt et al., 2018).

108 In view of this relative lack of information on the effects of non-steady state  
109 temperatures on biogeochemically important phytoplankton, we carried out a thermal  
110 variability study using the Sargasso Sea *E. huxleyi* isolate CCMP371. Our experiments  
111 combined ocean warming with thermal variations, with a focus on the increasing  
112 frequency of temperature variations under global climate change. We examined growth  
113 rates, photosynthesis, calcification and elemental composition under constant, one-day  
114 and two-day temperature variations. This study is intended to provide insights into how  
115 different frequencies of thermal variation may influence the physiology and  
116 biogeochemistry of this important marine calcifying phytoplankton species under both  
117 current and future sea surface temperatures.

#### 118 **Materials and methods**

119 The marine coccolithophore *E. huxleyi* (Lohm.) Hay and Mohler strain CCMP371  
120 (isolated from the Sargasso Sea) was maintained in the laboratory as stock batch  
121 cultures in Aquil medium ( $100 \mu\text{mol L}^{-1} \text{NO}_3^-$ ,  $10 \mu\text{mol L}^{-1} \text{PO}_4^{3-}$ ) made with  $0.2 \mu\text{M}$ -  
122 filtered coastal seawater collected from the California region (Sunda et al., 2005).  
123 Cells were grown at  $22^\circ\text{C}$  under  $120 \mu\text{mol photons m}^{-2} \text{s}^{-1}$  cool white fluorescent light  
124 with a 12 h/12 h light/dark cycle.

#### 125 **Experimental set-up**

126 An aluminum thermal gradient block with a range of 13 temperatures was used to  
127 perform the thermal response curve and temperature variation experiments. For the



128 thermal curve experiment, the extreme temperatures of the thermal-block were set to  
129 8.5 °C and 28.6 °C, with intermediate temperatures of 10.5 °C, 12 °C, 13.5 °C, 15.5 °C,  
130 17.5 °C, 18.5 °C, 21.3 °C, 22.6 °C, 24.5 °C, 26.6 °C, and 27.6 °C. The *E. huxleyi* cells  
131 were transferred from the stock cultures into triplicate 120 ml acid washed  
132 polycarbonate bottles in the thermal block under a 12 h light /12h dark cycle at 180  
133  $\mu\text{mol photons m}^{-2} \text{s}^{-1}$ .

134 Semi-continuous culturing methods were used for all experiments. Cultures were  
135 diluted every two days to keep them in exponential growth stage while acclimating to  
136 the treatment temperatures for two weeks. Dilution volumes were calculated to match  
137 growth rates of each individual replicate, as measured using in vivo chlorophyll a (Chl  
138 *a*) fluorescence. Once steady-state growth rates were recorded for 3–5 consecutive  
139 transfers, the cultures were sampled (Zhu et al., 2017). To estimate the negative growth  
140 rates observed at 28.6 °C, these cultures were diluted from 22 °C stock cultures, and  
141 sampled after 4-6 days for growth rates and elemental stoichiometry.

142 Six treatments were used to determine the responses of *E. huxleyi* growth,  
143 photosynthesis and calcification to different frequencies of temperature fluctuation.  
144 Temperature fluctuation treatments included: 1) Low temperature, constant (18.5  
145 °C). 2) Low temperature, one-day fluctuation cycle (16-21°C, mean = 18.5°C). 3) Low  
146 temperature, two-day fluctuation cycle (16-21°C, mean =18.5°C). 4) High temperature,  
147 constant (25.5 °C). 5) High temperature, one-day fluctuation cycle (23-28°C, mean =  
148 25.5°C). 6) High temperature, two-day fluctuation cycle (23-28°C, mean = 25.5°C).  
149 The experimental *E. huxleyi* cultures were grown in triplicate in 120 ml acid washed



150 polycarbonate bottles using the thermal-block under a 12 h light /12h dark cycle at 180  
151  $\mu\text{mol photons m}^{-2} \text{ s}^{-1}$ .

152 For the variable temperature experiment, cultures were diluted semi-continuously  
153 every two days for constant and one-day variation treatments, and every four days for  
154 two-day variation treatments.  $100 \mu\text{mol L}^{-1}$  nitrate and  $10 \mu\text{mol L}^{-1}$  phosphate was  
155 added every two days. Cultures were grown for at least eight dilutions (~16 days for  
156 constant and one day variation treatments; ~32 days for two-day variation treatments)  
157 to acclimate to the different experimental conditions before final sampling. All  
158 variation treatments were sampled twice across the thermal variation cycle, once  
159 during the cool phase and once during the warm phase.

#### 160 **Growth rates**

161 In vivo fluorescence was measured daily for the one-day variation treatment and  
162 every two days for the constant and two-day variation treatments using a Turner 10-  
163 AU fluorometer (Turner Designs, CA). In vivo-derived growth rates were  
164 subsequently verified using cell samples counted with a nanoplankton counting  
165 chamber on an Olympus BX51 microscope. Specific growth rates ( $\text{d}^{-1}$ ) were calculated  
166 using the in vivo fluorescence and cell count data as:  $\mu = \ln[N(T_2)/N(T_1)]/(T_2 - T_1)$ , in  
167 which  $N(T_1)$  and  $N(T_2)$  are the in vivo fluorescence values or cell counts at  $T_1$  and  $T_2$ .

#### 168 **Chl *a* analysis**

169 Twenty ml culture samples were filtered onto GF/F glass fiber filters (Whatman  
170 GFC, Maidstone, UK) for Chl *a* analysis. In vitro Chl *a* was extracted with 90%  
171 aqueous acetone for 24 hours at  $-20 \text{ }^\circ\text{C}$ , and then measured using a Turner 10-AU



172 fluorometer (Turner Design, USA). (Fu et al., 2007).

### 173 **Elemental analysis**

174 Elemental composition sampling included Total Particulate Carbon (TPC),  
175 Particulate Organic Carbon (POC), Particulate Organic Nitrogen (PON), Particulate  
176 Inorganic Carbon (PIC) and Particulate Organic Phosphorus (POP), allowing  
177 calculation of cellular elemental stoichiometry and calcite/organic carbon ratios  
178 (PIC/POC) (Feng et al.; 2008). Culture samples for TPC, POC and PON, were  
179 collected onto pre-combusted GF/F glass fiber filters (Whatman) and dried in a 60 °C  
180 oven overnight. For POC analysis, filters were fumed for 24 hours with saturated  
181 HCl to remove all inorganic carbon prior to analysis. TPC, PON and POC were then  
182 measured by a 440 Elemental Analyzer (Costech Inc, CA) following Fu et al. (2007).  
183 PIC was calculated as the difference between TPC and POC. For POP measurement,  
184 culture samples were filtered on onto pre-combusted GF/F filters (Whatman) and  
185 analyzed using a molybdate colorimetric method according to Fu et al. (2007).

### 186 **Total carbon fixation, photosynthetic and calcification rates & ratios**

187 Total carbon fixation, photosynthetic carbon fixation and calcification rates were  
188 measured using  $^{14}\text{C}$  incubation techniques (Feng et al., 2008). Sixty mL culture  
189 samples from each treatment were spiked with 0.2  $\mu\text{Ci NaH}^{14}\text{CO}_3$  and then incubated  
190 for 4 h under their respective experimental conditions. After incubation, samples were  
191 filtered on two Whatman GF/F filters (30mL each) for total carbon fixation and  
192 photosynthetic rate separately. The filters for photosynthetic rate measurement were  
193 fumed with saturated HCl before adding scintillation fluid. Thirty mL from each



194 treatment (10 mL from each replicate bottle) was filtered immediately, after adding  
195 equal amounts of  $\text{NaH}^{14}\text{CO}_3$  for procedural filter blanks. Filters were then placed in 7  
196 mL scintillation vials with 4 mL scintillation fluid overnight in the dark. To determine  
197 the total radioactivity (TA), 0.2  $\mu\text{Ci}$   $\text{NaH}^{14}\text{CO}_3$  together with 100  $\mu\text{L}$  phenylalanine  
198 was placed in scintillation vials with the addition of 4 mL scintillation solution. All  
199 samples were counted on a Perkin Elmer Liquid Scintillation Counter to measure the  
200 radioactivity. Total carbon fixation and photosynthetic rate were calculated from TA,  
201 final radioactivity and total dissolved inorganic carbon (DIC) values. Calcification rate  
202 was then calculated as the difference between total carbon fixation and photosynthetic  
203 rate for each sample.

#### 204 **Model for population growth of *E. huxleyii***

205 Growth rates measured under constant temperatures in the thermal block were  
206 fitted to the Eppley thermal performance curve or TPC (Eppley, 1972; Norberg, 2004;  
207 Thomas et al., 2012). This function quantifies parameters of growth temperature  
208 effects, including the temperature optimum for growth ( $T_{\text{opt}}$ ), and high and low  
209 temperature limits ( $T_{\text{max}}$  and  $T_{\text{min}}$  respectively) in our strain of *E. huxleyii*. A modified  
210 version of this equation was also plotted to predict the impact that fluctuating  
211 temperatures might have on growth rates at present-day and future mean temperatures  
212 (Bernhardt et al., 2018, Kling et al. in review, Qu et al. in review).

#### 213 **Statistical analysis**

214 The mean values of most parameters measured under the variation treatments were  
215 calculated by averaging the values from the cool and warm phases, including all the



216 elemental content and ratios, photosynthetic and calcification rates and ratios. All  
217 statistical analyses, including student t-tests and ANOVA were conducted using the  
218 open source statistical software R version 3.5.0 (R Foundation).

## 219 **Results**

### 220 **Responses of *E. huxleyi* to warming**

221 The growth rates of *E. huxleyi* at constant temperature increased significantly with  
222 warming from  $0.09 \pm 0.01 \text{ d}^{-1}$  at  $8.5 \text{ }^\circ\text{C}$  to a maximum value of  $0.90 \pm 0.02 \text{ d}^{-1}$  at  $21.3 \text{ }^\circ\text{C}$ .  
223 Growth was optimal up to  $24.5 \text{ }^\circ\text{C}$ , and then decreased rapidly to  $-0.46 \pm 0.05 \text{ d}^{-1}$  at  $28.6$   
224  $^\circ\text{C}$  ( $p < 0.05$ , Fig. 1).

225 The elemental ratios of the cells in the different temperature treatments were  
226 compared to the average elemental ratios across the entire temperature range (Fig. 2).  
227 The thermal trends of TPC/PON ratios were generally similar with those of growth  
228 rates, in that ratios increased from  $8.5$  to  $17.5 \text{ }^\circ\text{C}$ , and then decreased from  $24.5$  to  $27.6$   
229  $^\circ\text{C}$ . The TPC/PON ratios at  $8.5$ ,  $10.5$  and  $27.6 \text{ }^\circ\text{C}$  were significantly lower than the  
230 average level of all the temperature points ( $p < 0.05$ , Fig 2A). The POC/PON ratios of  
231 most temperature points were very close to the mean value of  $6.3$ , except at  $27.6 \text{ }^\circ\text{C}$   
232 ( $7.1$ ) and  $28.6 \text{ }^\circ\text{C}$  ( $7.4$ ), which were significantly higher than the average ( $p < 0.05$ , Fig  
233 2B). The highest PIC/POC ratio was  $0.49 \pm 0.07$  at  $22.6 \text{ }^\circ\text{C}$ , and the lowest PIC/POC  
234 ratio was  $0.05 \pm 0.04$  at  $27.6 \text{ }^\circ\text{C}$ , a value that was almost 90% less than the highest value.  
235 The PIC/POC ratios at the lowest temperature tested ( $10.5 \text{ }^\circ\text{C}$ ) and at the high end of  
236 the temperature range ( $26.6$  and  $27.6 \text{ }^\circ\text{C}$ ) were significantly lower than the average  
237 level (Fig. 2C). Chl *a*/POC ratios were significant lower at  $8.5$ ,  $10.5$  and  $27.6 \text{ }^\circ\text{C}$  than



238 the mean, and at 17.5, 21.3, 22.6 and 24.5 °C were significantly higher than the average  
239 ( $p < 0.05$ , Fig. 2C). The trends of PIC/POC and Chl *a*/POC ratio were similar, in that  
240 they gradually increased from low temperature and to the highest value at 22.6 °C, and  
241 then dropped rapidly as temperature increased further. (Fig. 2C, D).

## 242 Responses of *E. huxleyi* to temperature variations

### 243 Growth rate

244 In low temperature experiments, both one-day and two-day temperature variations  
245 had a negative effect on growth rate. The mean growth rates of the one-day  
246 ( $0.71 \pm 0.01 \text{ d}^{-1}$ ) and two-day ( $0.72 \pm 0.01 \text{ d}^{-1}$ ) variation treatments were not significantly  
247 different from each other ( $p > 0.05$ ), but both were lower than that of the constant 18.5  
248 °C treatment ( $0.76 \pm 0.01$ ,  $p < 0.05$ ) (Fig. 3A). Growth rates were low during the cool  
249 phase (16 °C) of the experiment ( $\sim 0.5\text{-}0.6 \text{ d}^{-1}$ ), but those of the two-day variation cycle  
250 were not significantly different from the constant control at this temperature ( $p > 0.05$ ).  
251 However, the cool phase of the one-day variation cycle had growth rates were lower  
252 than those of the constant 16 °C treatment ( $p < 0.05$ ). During the warm phase of the  
253 thermal cycle (21°C), there were no significant differences in the elevated growth rates  
254 ( $\sim 0.85\text{-}0.9 \text{ d}^{-1}$ ) of the constant control and those of either variable treatment ( $p > 0.05$ ,  
255 Fig. 3A).

256 In the high temperature experiments, as in the low temperature experiments, both  
257 temperature variation frequencies had a negative effect on mean growth rates. The  
258 growth rates in the two-day variation treatment were ( $0.20 \pm 0.02 \text{ d}^{-1}$ ), a decrease of  
259  $\sim 74\%$  compared with the constant 25.5 °C ( $p < 0.05$ ), and  $\sim 62\%$  of the one-day



260 variation treatment value ( $p < 0.05$ , Fig. 3B). During the cool phase ( $23\text{ }^{\circ}\text{C}$ ), the growth  
261 rate of the one-day variation treatment was slightly lower ( $p < 0.05$ ) than the constant  
262  $23\text{ }^{\circ}\text{C}$ , but there were no significant changes between two-day variations and the  
263 constant  $23\text{ }^{\circ}\text{C}$  treatment ( $p > 0.05$ , Fig. 3B). During the warm phase ( $28\text{ }^{\circ}\text{C}$ ), the  
264 constant  $28\text{ }^{\circ}\text{C}$  and two-day variation treatment both had negative growth rates of -  
265  $0.45 \pm 0.05\text{ d}^{-1}$  and  $-0.45 \pm 0.04\text{ d}^{-1}$ , respectively. However, the one-day variation  
266 treatment had a low but positive warm phase growth rate at  $0.25 \pm 0.02\text{ d}^{-1}$  (Fig. 3B).

#### 267 **Cellular PIC and POC contents and ratios**

268 In low temperature experiments, the cellular PIC content of the constant  $18.5\text{ }^{\circ}\text{C}$   
269 treatment was  $3.5 \pm 0.3\text{ pg/cell}$ , and there were no significant differences with  
270 temperature variation treatments ( $p > 0.05$ , Table 1). However, the cellular POC  
271 content of the constant  $18.5\text{ }^{\circ}\text{C}$  treatment was  $8.0 \pm 0.6\text{ pg/cell}$ , which was lower than  
272 in the two-day variation treatment, but significantly higher than in the one-day  
273 variation treatment ( $p < 0.05$ ).

274 Like POC, the PIC/POC ratio was significantly affected by temperature variations  
275 (Fig. 4A). The lowest PIC/POC ratio was found in the one-day variation treatment  
276 ( $0.38 \pm 0.07$ ), which was significantly lower than the two-day variation treatment value  
277 ( $p < 0.05$ ), but close to that in the constant  $18.5\text{ }^{\circ}\text{C}$  ( $p > 0.05$ ). A similar trend was  
278 found in both the cool ( $16\text{ }^{\circ}\text{C}$ ) and warm phases ( $21\text{ }^{\circ}\text{C}$ ) of the two variation treatments,  
279 in that the PIC/POC ratio of the one-day variation treatment was lower than of the  
280 two-day variation treatment ( $p < 0.05$ , Fig. 4A). Both variation treatments had lower  
281 PIC/POC ratios during the warm phase than during the cool phase, although these



282 differences were not significant ( $p > 0.05$ ).

283 High temperature experiments showed particulate carbon trends that were contrary  
284 to those of the low temperature treatments. The PIC content and PIC/POC ratios were  
285 significantly decreased by temperature variation. The cellular PIC content of the  
286 constant treatment (25.5 °C) was  $5.5 \pm 0.3$  pg/cell, which was ~ 200% higher than that  
287 of the one-day variation and ~ 160% higher than in the two-day variation treatments  
288 ( $p < 0.05$ , Table 1). The same trend was found for PIC/POC ratios in one-day variation  
289 and two-day variation treatments, which decreased ~ 67% and 33% compared with the  
290 constant 25.5 °C treatment, respectively ( $p < 0.05$ , Fig. 4B). However, the POC content  
291 of one-day and two-day variation treatments was higher than in the constant 25.5 °C  
292 treatment ( $p < 0.05$ , Table 1). During the cool phase (23 °C), the PIC content and  
293 PIC/POC ratio of the one-day variation treatment was significantly lower than in the  
294 two-day variation treatment, but contrary to PIC content, the POC content of the one-  
295 day variation treatment was significantly higher than that in the two-day variation  
296 treatment. During the warm phase (28 °C), there were no significant differences of PIC  
297 content, POC content, or PIC/POC ratio between the one-day and two-day variation  
298 treatments (Fig. 4B, Table 1).

### 299 **Photosynthetic and calcification rates and ratios**

300 In low temperature treatments, there were no differences between total carbon  
301 fixation rates (photosynthesis plus calcification) for the two variable treatments  
302 relative to the constant control (Fig. 5A). However, during the cool phase total  
303 carbon fixation rates were higher in the one-day variation than in the two-day variation



304 (p<0.05, Fig 5A), while this rate was the same in both variation treatments during the  
305 warm phase (p > 0.05, Fig. 5A). In high temperature experiments, the total carbon  
306 fixation rates of the one-day and two-day variation treatments were significantly  
307 decreased by about ~20% and ~18% respectively, compared with the constant 25.5 °C  
308 treatment (p<0.05, Fig. 5 B).

309 The photosynthetic and calcification rates of the constant 18.5 °C treatment were  
310  $0.04\pm 0.00$  pmol C cell<sup>-1</sup> hr<sup>-1</sup> and  $0.02\pm 0.00$  pmol C cell<sup>-1</sup> hr<sup>-1</sup>, respectively, which were  
311 not significantly different from both of the temperature variation treatments (p > 0.05,  
312 Fig. 5 C,E). Photosynthetic rates changed within the thermal cycle for both one-day  
313 and two-day variation treatments, with a decrease of 22% and 28% from the warm  
314 phase to the cool phase, respectively (Fig. 5C). However, there were no significant  
315 changes in calcification rates under either variation frequency treatment between the  
316 cool and warm phases of the thermal cycles (p > 0.05).

317 In the mean 25.5 °C experiment, photosynthetic rates were not significantly  
318 different between the one-day variation and constant treatments (p > 0.05), while the  
319 photosynthetic rate of the two-day variation was slightly higher than that of the  
320 constant 25.5 °C treatment (p<0.05, Fig. 5D). In contrast, calcification rates of one-  
321 day and two-day variation treatments at a mean temperature of 25.5 ° were  
322 significantly decreased by about ~46% and ~51%, respectively, relative to the constant  
323 control (p<0.05, Fig. 5F). There were no significant differences in total carbon fixation,  
324 photosynthetic and calcification rates between the one-day variation and two-day  
325 variation treatments during both the cool (23 °C) and warm (28 °C) phases (p>0.05,



326 Fig. 5 B,D,F).

327 In the low temperature treatments, there were no significant differences in  
328 Cal/Photo ratios between the constant and the two variable treatments ( $p > 0.05$ , Fig  
329 6A). In contrast, in the high temperature experiments, the Cal/Photo ratio of the one-  
330 day variation and two-day variation treatments were decreased by ~40% and 49%,  
331 respectively, compared with the constant 25.5 °C treatment ( $p < 0.05$ , Fig. 6B). For both  
332 low and high temperature experiments, there were no significant differences between  
333 the one-day and two-day variation treatments in either the cool or warm phases of the  
334 thermal cycle ( $p > 0.05$ , Fig. 6B). However, in both temperature treatments the lower  
335 photosynthetic rates during the cool phase (Fig. 5C,D) resulted in an increase in the  
336 Cal/Photo ratio during the cool phase for both the one-day and two-day variation  
337 treatments ( $p < 0.05$  Fig. 6A,B).

338

### 339 **Elemental content and stoichiometry**

340 In the low temperature experiments, the one-day variation and two-day thermal  
341 variations had different effects on cellular elemental contents and ratios, relative to the  
342 constant 18.5 °C treatment. One-day variation increased most of the cellular elemental  
343 and biochemical contents (TPC, PON, and Chl *a*) but with no significant difference  
344 ( $p > 0.05$ ), except for POP content ( $p < 0.05$ ), compared with the constant 18.5 °C  
345 treatment (Table 1). In contrast, the two-day variation treatment decreased all the  
346 measured cellular elemental and biochemical contents (TPC, PON, POP and Chl *a*,  
347  $p < 0.05$ ) in relation to the constant 18.5 °C treatment (Table 1). However, the



348 TPC/PON and Chl *a*/POC ratios of the two-day variation treatment were higher than  
349 those of the one-day variation and constant 18.5 °C treatments ( $p < 0.05$ , Fig. 7A,E),  
350 while the PON/POP ratio was lower than in the one-day variation and constant 18.5  
351 °C treatments ( $p < 0.05$ , Fig. 7C). There were no significant differences in TPC/PON,  
352 PON/POP and Chl *a*/POC ratios between the constant 18.5 °C and the one-day  
353 variation treatments ( $p > 0.05$ , Fig. 7A).

354 In high temperature experiments, the highest cellular TPC, PON and POP contents  
355 were all obtained under the one-day variation treatment, which was significantly  
356 higher than under constant 25.5 °C conditions ( $p < 0.05$ , Table 1). However, there were  
357 no significant differences in cellular Chl *a* content between the constant 25.5 °C and  
358 both variation treatments ( $p > 0.05$ , Table 1). The TPC/PON ratio of the constant 25.5  
359 °C treatment was ~22% and ~35% higher than that of the two-day variation and one-  
360 day variation treatments, respectively ( $p < 0.05$ , Fig. 7B), while the PON/POP ratio was  
361 highest in the day variation, followed by the two-day variation and finally by the  
362 constant control (Fig. 7D). The Chl *a*/POC ratio of the one-day variation treatment  
363 was significantly lower than that of the constant 25.5 °C and two-day variation  
364 treatments ( $p < 0.05$ ), but there were no significant differences between the constant  
365 25.5 °C and two-day variation treatments ( $p > 0.05$ , Fig. 7F).

366 During the cool phase of the high temperature experiments (23 °C), the cellular  
367 TPC, PON, POP and Chl *a* content of two-day variation were all significantly lower  
368 than in the one-day variation treatment ( $p < 0.05$ ). Similar decreasing trends during the  
369 cool phase were observed for the TPC/PON ratios (Fig. 7B), but not the Chl *a*/POC



370 ratio, which was ~32% higher than in the one-day variation treatment ( $p < 0.05$ , Fig.  
371 7F). During the warm phase (28 °C), there were no significant differences of cellular  
372 TPC, PON and POP contents between one-day and two-day variation treatments ( $p >$   
373 0.05, Table 1) as well as the TPC/PON ratio (Fig 7B). However, the Chl *a* content of  
374 the one-day variation treatment was ~20% lower than that of the two-day variation  
375 treatment ( $p < 0.05$ ). The Chl *a*/POC ratio was not significantly different between the  
376 one-day and two-day variation treatments at the warm phase ( $p > 0.05$ , Table 1, Fig.  
377 7F).

#### 378 **Experimental constant temperature performance curves and measured and** 379 **modeled fluctuating temperature TPCs**

380 The experimentally-determined constant condition TPCs and the predicted  
381 fluctuating temperature condition TPCs based on the Eppley thermal performance  
382 curve are shown in Fig. 8 for *E. huxleyi*. Compared with the measured TPC under  
383 constant thermal conditions, the modeled TPC of the fluctuating temperature condition  
384 showed a leftward shift towards lower temperatures at optimum temperatures and  
385 above. The maximum and optimal temperature of the modeled fluctuating temperature  
386 TPC were all lower than those of the measured constant condition TPC. In particular,  
387 the optimal temperature for growth decreased from 22°C in constant conditions to 21  
388 °C under fluctuating temperature conditions. At the same time, the maximum growth  
389 rate ( $\mu_{\max}$ ) of the fluctuating temperature condition was 0.8 d<sup>-1</sup>, which was lower than  
390 the constant condition value of 0.9 d<sup>-1</sup>. The measured growth rates of experimental  
391 one-day (0.71 d<sup>-1</sup>) and two-day (0.72 d<sup>-1</sup>) variation treatments at the relatively low



392 mean temperature of 18.5 °C closely matched the model-predicted fluctuating  
393 temperature growth rate at this temperature ( $0.74^{-1}$ , Fig. 8). However, measured and  
394 predicted growth rates did not match as well at the higher mean temperature. At 25.5  
395 °C, the measured growth rate of the one-day variation was  $0.52 \text{ d}^{-1}$ , 30% higher than  
396 the predicted fluctuating temperature growth rate of  $0.40 \text{ d}^{-1}$ . In contrast, the measured  
397 growth rate of the experimental two-day variation treatment was  $0.20 \text{ d}^{-1}$ , a decrease  
398 of 50% compared to the model-predicted fluctuating temperature growth rate of  $0.40$   
399  $\text{d}^{-1}$  at this temperature (Fig. 8).

#### 400 Discussion

##### 401 Effects of warming on *Emiliana huxleyi* growth rates and elemental ratios

402 Thermal response curves and optimum growth temperatures describe the  
403 importance of temperature as a control on the distribution of *E. huxleyi* strains in the  
404 ocean (Buitenhuis et al., 2008; Paasche, 2001). The optimal temperature range of 21.3-  
405 24.5 °C found in our study is similar to that of some other *E. huxleyi* strains (De Bodt  
406 et al., 2010; Feng et al., 2017; Rosas-Navarro et al., 2016). Most studies have focused  
407 on the lower part of the temperature curve where growth rates increase with rising  
408 temperatures, with relatively few examining stressfully warm temperatures where  
409 growth is inhibited (Feng et al., 2017; Matson et al., 2016). In our study, the descending  
410 portion of the upper TPC ranged from 24.5 °C to 28.6 °C, at which point growth rates  
411 became negative. This *E. huxleyi* strain was isolated from the Sargasso Sea where the  
412 sea surface temperature can reach 29 °C in the summer, and will be higher in the future  
413 with global warming (<https://seatemperature.info/sargasso-sea-water->



414 temperature.html). This suggests that this strain may be currently living near its upper  
415 thermal limit for part of the year, as are many other tropical and subtropical  
416 phytoplankton (Thomas et al. 2012), and that it may therefore be vulnerable to further  
417 warming.

418 Calcification is the key biogeochemical functional trait of this species, and the  
419 PIC/POC ratio of *E. huxleyi* can be influenced by factors that include CO<sub>2</sub> concentration,  
420 nutrient status, irradiance and temperature (Feng et al., 2008, 2017; Raven & Crawford,  
421 2012). The cellular PIC/POC of *E. huxleyi* has been reported to decrease as irradiance  
422 and CO<sub>2</sub> concentration rises, but increase under nitrate and phosphate limitation (Feng  
423 et al., 2017; Paasche, 1999; Riegman et al., 2000). The effect of temperature on *E.*  
424 *huxleyi* cellular PIC/POC ratio is however more complex. De Bodt et al. (2010) and  
425 Gerecht et al. (2014) observed that higher cellular PIC/POC ratios were obtained at  
426 lower temperatures for both *E. huxleyi* and *Coccolithus pelagicus*. Sett et al. (2014),  
427 however, found an opposite trend, whereby the PIC/POC ratio increased with  
428 temperature in another strain of *E. huxleyi*. Feng et al. (2017) reported that the cellular  
429 PIC/POC of *E. huxleyi* was increased as the temperature rose from 4 °C to 11 °C, but  
430 decreased with warming from 11 °C to 15 °C and remained steady afterwards.

431 In our study, the cellular PIC/POC ratio of *E. huxleyi* was positively correlated to  
432 growth rate ( $R^2=0.73$ ), and increased with warming from 8.5 °C to a maximum at 22.6  
433 °C, and then decreased with further warming to 27.6 °C. In a meta-analysis of studies  
434 using different coccolithophore subgroups, Krumhardt et al. (2017) found that the  
435 highest PIC/POC ratios were observed between 15 °C and 20 °C, in the same thermal



436 range where the highest growth rates of *E. huxleyi* are found, as seen here and in Sett  
437 et al. (2014). In contrast, Rosas-Navarro et al. (2016) reported that the cellular PIC/POC  
438 ratio showed a minimum at optimal growth temperature (between 20 and 25 °C) for  
439 three strains of *E. huxleyi*. However, the *E. huxleyi* strain used here was isolated from  
440 a warmer area (the Sargasso Sea) compared with isolates from coastal Japan and New  
441 Zealand in previous studies (Rosas-Navarro et al. 2016; Feng et al. 2017). The growth  
442 temperature for our stock cultures was 22-24°C, higher than that of the other two *E.*  
443 *huxleyi* strains. Feng et al. (2017) also found that the optimal temperature for  
444 calcification was close to the stock culture maintenance temperature in their study. Our  
445 results also support suggestions that stressful high temperatures may lead to decreases  
446 in cellular PIC/POC ratios and calcification (De Bodt et al., 2010; Feng et al., 2017;  
447 Gerecht et al., 2014; Krumhardt et al., 2017).

448 The cellular Chl *a*/POC ratio of *E. huxleyi* showed a similar pattern with the  
449 PIC/POC ratio, as it was also positively correlated to growth rate. Zhu et al. (2017)  
450 reported the cellular Chl *a*/POC ratio of a Southern California diatom was also  
451 correlated to growth rate across a very similar temperature range. In contrast, Feng et  
452 al. (2017) found that the cellular Chl *a*/POC ratio of *E. huxleyi* dramatically decreased  
453 with warming. However, in our experiments, the cellular Chl *a*/POC ratio was lower at  
454 27.6 °C than at 28.6 °C, likely due to the negative growth rates and consequent lack of  
455 acclimation of the cultures maintained at the highest temperature. Traits such as  
456 PIC/POC ratios, Chl *a*/POC ratios and TPC/PON ratios also showed some evidence for  
457 possible carryover from the stock cultures (22-24 °C) in this 28.6 °C treatment, as we



458 were forced to sample before the cells died completely, after only 2-3 cycles of dilution.

## 459 **Effect of thermal variation on *Emiliana huxleyi* growth and physiology**

### 460 ***Constant vs variable temperature***

461 Thermal variability in the surface ocean is becoming an increasingly relevant  
462 topic as global warming proceeds. In our study, we found that the growth rates of a  
463 subtropical *E. huxleyi* strain were quite sensitive to temperature variation under both  
464 low (18.5 °C, “winter”) and high (25.5 °C, “summer”) mean temperatures. In both low  
465 and high temperature experiments, growth rates always decreased under temperature  
466 variation, compared with the constant mean temperature. This result agrees with  
467 previous studies showing that temperature variation slowed the growth rates of the  
468 fresh water green alga *Chlorella pyrenoidosa* and the marine diatom *Cyclotella*  
469 *meneghiniana*, as observed in laboratory work but also during long-term field  
470 observations (Zhang et al., 2016).

471 This growth rate inhibition under temperature variation was more pronounced at  
472 high temperature than at low temperature, indicating that variability at the warm range  
473 boundary will have a stronger negative effect on population growth rate than  
474 variability near the lower thermal limits (Bernhardt et al., 2018). This trend suggests  
475 that high temperatures, whether constant or variable, can in general irreversibly  
476 damage key cellular biochemical pathways and so inhibit growth rate. However,  
477 following Jensen’s inequality model to predict the thermal performance curve, there  
478 should be an inflection point where the transfer between positive and negative effects  
479 of temperature variability will occur compared with the constant thermal curve.



480 Conversely, for phytoplankton living in regions of suboptimal temperatures, thermal  
481 variation can enhance growth (Bernhardt et al., 2018). Thus, for some polar  
482 phytoplankton or for temperate species extending their ranges poleward, such as *E.*  
483 *huxleyi* (Neukermans et al., 2018), not only warming but also thermal variability may  
484 need to be taken into consideration in order to understand changes in high latitude  
485 microbial communities and biogeochemistry cycles.

486 Temperature variation affected the physiology of *E. huxleyi* differently compared  
487 with constant temperature. Physiological traits that were affected by thermal  
488 fluctuations also differed at low temperature (“winter”) and high temperature  
489 (“summer”), suggesting different response mechanisms. Under low temperature  
490 variations (16-21 °C), photosynthesis and calcification were correlated with  
491 temperature, leading to rates similar to those observed with constant temperature.  
492 However, elemental contents and ratios under thermal variations differed from  
493 constant temperature. For instance, the cellular POC, PON, POP and Chl *a* contents  
494 increased during one-day variations but decreased during two-day variations,  
495 compared with constant temperature.

496 These cellular quota changes were reflected in elemental ratio differences  
497 (PIC/POC, Chl *a*/POC and TPC/POC) between the thermal variation treatments and  
498 constant temperature. However, the changes between thermal variation and constant  
499 treatments were not significant under low temperature (“winter”), indicating that the  
500 thermal variation wouldn’t significantly influence biogeochemical cycles under these  
501 conditions. Unlike constant temperature treatments where selection may favor a higher



502 growth rate, the trade-off for the thermal variation treatments may involve sacrificing  
503 increased growth rate in order to adjust cellular stoichiometry to adapt to the  
504 fluctuating environment.

505 In contrast, photosynthetic and calcification rates under high temperature thermal  
506 variations (23-28 °C) were significantly different from those seen under constant  
507 temperature (25 °C), especially the calcification rate. Thermal variation treatments  
508 transiently but repeatedly experienced the extreme high temperature point (28 °C),  
509 leading to extremely low calcification rates and PIC contents, and thus relatively low  
510 PIC/POC and Cal/Photo ratios. Previous *E. huxleyi* studies agree that high temperature  
511 decreases PIC content, PIC/POC ratios and Cal/Photo ratios (Feng et al., 2017; 2018;  
512 Gerecht et al., 2014). The two different patterns of responses to thermal variation we  
513 observed under low and high temperatures imply a seasonal pattern in the ways that  
514 thermal variations will affect the elemental stoichiometry of *E. huxleyi*.

515 Under other stresses such as nutrient limitation, trade-offs between growth rates  
516 and resource affinities may be necessary to adapt to thermal changes. For instance,  
517 nitrate affinity declines in cultures of the large centric diatom *Coscinodiscus*  
518 acclimated to warmer temperatures (Qu et al. 2018), while warming decreases cellular  
519 requirements for iron in the nitrogen-fixing cyanobacterium *Trichodesmium* (Jiang et  
520 al. 2018). In nitrogen-limited cultures of the marine diatom *Thalassiosira pseudonana*,  
521 long-term thermal adaptation acted most strongly on systems other than those involved  
522 in nitrate uptake and utilization (O'Donnell et al., 2018). Thus, it is possible that our  
523 thermal response results with *E. huxleyii* might have differed under nutrient-limited



524 growth conditions.

525 ***One-day vs two-day thermal variation***

526 As temperature fluctuations in the surface ocean increase along with climate  
527 change, phytoplankton will be influenced by the frequencies and intensities of these  
528 thermal excursions. We found that the responses of *E. huxleyi* to one-day versus two-  
529 day temperature variations were different at both low and high temperature. For  
530 instance, under low temperature the transition from the warm phase to the cool phase  
531 during the thermal variation could be treated as a low temperature stress leading to a  
532 lag phase in growth. The growth rate of the one-day variation treatment at the cool  
533 phase was lower than that of the two-day variation, suggesting that physiological  
534 acclimation is not rapid enough to accommodate to the shorter variation treatment,  
535 while the two day variation allows enough time for growth to recover. However, at the  
536 warm phase (21 °C) there was no difference in growth rates between the one-day and  
537 two-day variations compared with the constant 21-degree treatment. These results  
538 imply that there was a shorter lag phase after transfer at the optimal temperature point  
539 (21 °C at the warm phase) than during low temperature stress (16 °C at the cool phase).

540 There was no significant difference in photosynthetic rates between the one-day  
541 and two-day variation during the warm phase (21 °C), but both were higher than during  
542 the cool phase, indicating the photosynthetic rate was correlated to the thermal  
543 variation cycle. However, for the calcification rate there was no significant difference  
544 between one-day and two-day variations during either the cool or warm phases. These  
545 results suggested that photosynthesis was more responsive to temperature variations



546 than calcification, and so ultimately determined the growth rate in both cool and warm  
547 phases. Feng et al. (2017) reported a similar relationship between growth and  
548 photosynthetic rates of a Southern Hemisphere *E. huxleyi* cultured at different  
549 temperatures.

550 Temperature variation frequencies also strongly influenced elemental  
551 composition. In low temperature experiments, the cellular contents of PON, POP and  
552 POC in the one-day variation treatment were all higher than under two-day variations.  
553 A notable exception to this trend was the cellular PIC content, which was not  
554 significantly different between one-day and two-day variation treatments. The PIC  
555 content was positively correlated to calcification and relatively stable, indicating that  
556 coccolith production and storage of *E. huxleyi* was relatively independent of the  
557 frequency of thermal variation.

558 Unlike the photosynthetic rate, the cellular elemental content of one-day and two-  
559 day variations were significantly different, but were not changed during temperature  
560 variation when transitioning from the warm phase to the cool phase or vice versa.  
561 The temperature dependent photosynthetic enzyme activity likely determined the  
562 similar photosynthetic rate of one-day and two-day variation treatments at both cool  
563 and warm phase in our short-term experiment, but the divergent responses of cellular  
564 stoichiometry in one-day and two-day thermal variations indicated different  
565 mechanisms of rapid acclimation to different thermal fluctuation frequencies. Our  
566 results imply that the responses of *E. huxleyi* to one-day and two-day thermal  
567 variations have different patterns, but both reach stable states during extended periods



568 of temperature fluctuation. Due to decreasing POC content, the PIC/POC ratio  
569 increased in the two-day variation compared with the one-day variation, suggesting  
570 that more rapid thermal fluctuations might lead to a decrease in calcite ballasting of  
571 sinking organic carbon.

572 Under the high temperature scenario, thermal variation forces the microalgae to  
573 intermittently deal with a lethal high temperature during the warm phase (28 °C), with  
574 potentially irreversible damage to the cells. In the “summer” experiments, the mean  
575 growth rate of the two-day variation was much lower than that of the one-day variation.  
576 This mainly resulted from the negative growth rate of two-day variation cultures  
577 during the warm phase (28 °C), whereas the growth rate of the one-day variation  
578 was  $>0.20 \text{ d}^{-1}$ . This result demonstrates that high frequency temperature variations  
579 (one-day) can partly mitigate growth inhibition by high temperatures in *E. huxleyi*, and  
580 so allow tolerance to extreme thermal events relative to longer exposures. This  
581 observation agrees with previous studies of other marine organisms such as corals  
582 (Oliver & Palumbi, 2011; Safaie et al., 2018). In the case of our experiments, the lag  
583 phase and metabolic inertia would help to maintain the microalgae during short  
584 exposures (one-day) to high temperature when transitioning from the cool phase (23  
585 °C) to the warm phase (28 °C).

586 Likewise, the particulate organic element contents (PON, POP and POC) of *E.*  
587 *huxleyi* were more stable in one-day than in two-day temperature variation treatments.  
588 The relatively steady status of cellular particulate organic matter content in the high  
589 frequency temperature variation treatment may conserve energy, compared to the



590 energy-intensive redistribution of major cellular components under lower frequency  
591 temperature variations. This differential energetic cost may help to explain the  
592 differences in growth rates between the two treatments. Adaptation to high  
593 temperature may also require higher investment in repair machinery, such as heat shock  
594 proteins, leading to an increased demand for nitrogen and other nutrients, thus  
595 increasing cellular POC, PON and POP contents (O'Donnell et al., 2018).

#### 596 **Prediction and modelling of *E. huxleyi* responses to thermal variation**

597 Mathematical curves based on population growth rates from laboratory studies  
598 have been used to predict future population abundance, persistence or fitness in a  
599 changing world (Bernhardt et al., 2018; Deutsch et al., 2008; Jiang et al. 2017). We  
600 applied a modified version of the Eppley thermal performance curve to predict the  
601 influence of thermal variation on the growth rate of *E. huxleyi* (Fig. 8). *E. huxleyi*  
602 growth rates were predicted to be much lower at warmer temperatures under variable  
603 conditions compared to constant conditions, but there were no significant differences  
604 at cooler temperatures. Thus, the effect of thermal variation on population growth at  
605 the upper thermal limit was predicted to be stronger than that in the lower portion of  
606 the thermal range (Bernhardt et al., 2018; Sunday et al., 2012). This phenomenon has  
607 been widely observed in ectothermic taxa (Dell et al., 2011), but this model for the  
608 effect of thermal variation on population growth rate may lack the ability to predict  
609 species responses at the extreme edges of their ranges (Bernhardt et al., 2018).

610 Our results showed that the measured effects of a variable thermal regime on *E.*  
611 *huxleyi* growth rate fitted well with model-predicted values at a relatively low



612 temperature (mean=18.5 °C), but differed considerably at high temperature (mean=25.5  
613 °C). This was especially evident under the two-day variation conditions at a mean of  
614 25.5 °C, where the growth rate was sharply lower than predicted from the constant  
615 TPCs-based model. This result suggests that transient heat waves may erode thermal  
616 tolerances of *E. huxleyi* populations already growing near their upper thermal limits,  
617 and that the frequency and duration of such extreme events is critically important in  
618 determining the magnitude of this stress. This sensitivity to increased thermal  
619 variability may reduce the fitness of *E. huxleyi* in the future subtropical and tropical  
620 oceans.

621       Although thermal variation at high temperature negatively impacted the growth  
622 rate of *E. huxleyi* in our experiment, our relatively short-term study didn't address the  
623 potential for *E. huxleyi* to evolve under selection by frequent extreme heat events.  
624 Evolutionary change in the thermal optimum and the maximum growth temperature in  
625 response to ocean warming may reduce heat-induced mortality, and mitigate some  
626 ecological impacts of global warming (O'Donnell et al., 2018, Thomas et al., 2012). For  
627 example, Schlüter et al. (2014) found that after one year of experimental adaptation to  
628 warming (26.3°C), the marine coccolithophore *E. huxleyi* evolved a higher growth rate  
629 when assayed at the upper thermal tolerance limit. Similar results were reported for the  
630 marine diatom *Thalassiosira pseudonana* in recent studies (O'Donnell et al., 2018;  
631 Schaum et al., 2018). Schaum et al. (2018) also found that the evolution of thermal  
632 tolerance in marine diatoms can be particularly rapid in fluctuating environments.  
633 Furthermore, populations originating from more variable environments are generally



634 more plastic (Schaum & Collins, 2014; Schaum et al., 2013). Long-term evolutionary  
635 experiments with *E. huxleyi* will be necessary to determine how the thermal  
636 performance curve of this important marine calcifier may diverge under selection by  
637 different frequencies and durations of extreme thermal variation events.

638       Understanding the combination of ocean warming and magnified thermal  
639 variability may be a prerequisite to accurately predicting the effects of climate change  
640 on the growth and physiology of the key marine calcifier *E. huxleyi*. This information  
641 will help to inform biogeochemical models of the marine and global carbon cycles, and  
642 ecological models of phytoplankton distributions and primary productivity. How  
643 changing thermal variation frequencies will affect marine phytoplankton remains a  
644 relatively under-explored topic, but one that is likely to become increasingly important  
645 in the future changing ocean.

646



647 **Acknowledgements**

648 Support was provided by U.S. National Science Foundation Biological Oceanography  
649 grants OCE1538525 and OCE1638804 to F-XF and DAH. XW was supported by a  
650 grant from the China Scholarship Council.

651



652 **References**

- 653 Bernhardt, J. R., Sunday, J. M., Thompson, P. L., and O'Connor, M. I.: Nonlinear  
654 averaging of thermal experience predicts population growth rates in a thermally  
655 variable environment, *bioRxiv*, 247908, 2018.
- 656 Boyce, D. G., Lewis, M. R., and Worm, B.: Global phytoplankton decline over the past  
657 century, *Nature*, 466, 591, 2010.
- 658 Boyd, P., Dillingham, P., McGraw, C., Armstrong, E., Cornwall, C., Feng, Y.-y., Hurd,  
659 C., Gault-Ringold, M., Roleda, M., and Timmins-Schiffman, E.: Physiological  
660 responses of a Southern Ocean diatom to complex future ocean conditions, *Nature*  
661 *Climate Change*, 6, 207-216, <https://doi.org/10.1038/nclimate2811>, 2015.
- 662 Boyd, P. W., Strzepek, R., Fu, F., and Hutchins, D. A.: Environmental control of open-  
663 ocean phytoplankton groups: Now and in the future, *Limnol. Oceanogr.*, 55, 1353-  
664 1376, <https://doi.org/10.4319/lo.2010.55.3.1353>, 2010.
- 665 Boyd, P. W., Collins, S., Dupont, S., Fabricius, K., Gattuso, J. P., Havenhand, J.,  
666 Hutchins, D. A., Riebesell, U., Rintoul, M. S., and Vichi, M.: Experimental  
667 strategies to assess the biological ramifications of multiple drivers of global ocean  
668 change—A review, *Glob. Chang. Biol.*, 24, 2239-2261, [https://doi.org/](https://doi.org/10.1111/gcb.14102)  
669 [10.1111/gcb.14102](https://doi.org/10.1111/gcb.14102), 2018.
- 670 Bozinovic, F., Bastías, D. A., Boher, F., Clavijo-Baquet, S., Estay, S. A., and Angilletta  
671 Jr, M. J.: The mean and variance of environmental temperature interact to  
672 determine physiological tolerance and fitness, *Physiol. Biochem. Zool.*, 84, 543-  
673 552, <https://doi.org/10.1086/662551>, 2011.



- 674 Buitenhuis, E. T., Pangerc, T., Franklin, D. J., Le Quéré, C., and Malin, G.: Growth  
675 rates of six coccolithophorid strains as a function of temperature, *Limnol.*  
676 *Oceanogr.*, 53, 1181-1185, [https://doi.org/ 10.4319/lo.2008.53.3.1181](https://doi.org/10.4319/lo.2008.53.3.1181), 2008.
- 677 Burgmer, T., and Hillebrand, H.: Temperature mean and variance alter phytoplankton  
678 biomass and biodiversity in a long-term microcosm experiment, *Oikos*, 120, 922-  
679 933, <https://doi.org/2011>.
- 680 Cáceres, C. E.: Temporal variation, dormancy, and coexistence: a field test of the  
681 storage effect, *Proceedings of the National Academy of Sciences*, 94, 9171-9175,  
682 [https://doi.org/ 10.2307/42576](https://doi.org/10.2307/42576), 1997.
- 683 De Bodt, C., Van Oostende, N., Harlay, J., Sabbe, K., and Chou, L.: Individual and  
684 interacting effects of pCO<sub>2</sub> and temperature on *Emiliania huxleyi* calcification:  
685 study of the calcite production, the coccolith morphology and the coccosphere size,  
686 *Biogeosciences*, 7, 1401-1412, [https://doi.org/ 10.5194/bg-7-1401-2010](https://doi.org/10.5194/bg-7-1401-2010), 2010.
- 687 Dell, A. I., Pawar, S., and Savage, V. M.: Systematic variation in the temperature  
688 dependence of physiological and ecological traits, *Proceedings of the National*  
689 *Academy of Sciences*, 108, 10591-10596, [https://doi.org/ 10.2307/27978658](https://doi.org/10.2307/27978658),  
690 2011.
- 691 Deutsch, C. A., Tewksbury, J. J., Huey, R. B., Sheldon, K. S., Ghalambor, C. K., Haak,  
692 D. C., and Martin, P. R.: Impacts of climate warming on terrestrial ectotherms  
693 across latitude, *Proceedings of the National Academy of Sciences*, 105, 6668-6672,  
694 [https://doi.org/ 10.1073/pnas.0709472105](https://doi.org/10.1073/pnas.0709472105), 2008.
- 695 Eppley, R. W.: Temperature and phytoplankton growth in the sea, *Fish. bull.*, 70, 1063-



- 696 1085, 1972.
- 697 Feng, Y., Warner, M. E., Zhang, Y., Sun, J., Fu, F.-X., Rose, J. M., and Hutchins, D. A.:
- 698 Interactive effects of increased pCO<sub>2</sub>, temperature and irradiance on the marine
- 699 coccolithophore *Emiliana huxleyi* (Prymnesiophyceae), *Eur. J. Phycol.*, 43, 87-98,
- 700 <https://doi.org/10.1080/09670260701664674>, 2008.
- 701 Feng, Y., Roleda, M. Y., Armstrong, E., Boyd, P. W., and Hurd, C. L.: Environmental
- 702 controls on the growth, photosynthetic and calcification rates of a Southern
- 703 Hemisphere strain of the coccolithophore *Emiliana huxleyi*, *Limnol. Oceanogr.*,
- 704 62, 519-540, <https://doi.org/10.1002/lno.10442>, 2017.
- 705 Feng, Y., Roleda, M. Y., Armstrong, E., Law, C. S., Boyd, P. W., and Hurd, C. L.:
- 706 Environmental controls on the elemental composition of a Southern Hemisphere
- 707 strain of the coccolithophore *Emiliana huxleyi*, *Biogeosciences*, 15, 581-595,
- 708 <https://doi.org/10.1002/lno.10442>, 2018.
- 709 Friedland, K. D., Mouw, C. B., Asch, R. G., Ferreira, A. S. A., Henson, S., Hyde, K. J.,
- 710 Morse, R. E., Thomas, A. C., and Brady, D. C.: Phenology and time series trends
- 711 of the dominant seasonal phytoplankton bloom across global scales, *Global Ecol.*
- 712 *Biogeogr.*, 27, 551-569, <https://doi.org/10.1111/geb.12717>, 2018.
- 713 Fu, F.-X., Yu, E., Garcia, N. S., Gale, J., Luo, Y., Webb, E. A., and Hutchins, D. A.:
- 714 Differing responses of marine N<sub>2</sub> fixers to warming and consequences for future
- 715 diazotroph community structure, *Aquat. Microb. Ecol.*, 72, 33-46, [https://doi.org/](https://doi.org/10.5194/bg-2019-179)
- 716 [10.5194/bg-2019-179](https://doi.org/10.5194/bg-2019-179), 2014.
- 717 Fu, F. X., Warner, M. E., Zhang, Y., Feng, Y., and Hutchins, D. A.: Effects of Increased



- 718 temperature and CO<sub>2</sub> on photosynthesis, growth, and elemental ratios in marine  
719 *Synechococcus* and *Prochlorococcus* (cyanobacteria) 1, *J. Phycol.*, 43, 485-496,  
720 [https://doi.org/ 10.1111/j.1529-8817.2007.00355.x](https://doi.org/10.1111/j.1529-8817.2007.00355.x), 2007.
- 721 Gao, K., Zhang, Y., and Häder, D.-P.: Individual and interactive effects of ocean  
722 acidification, global warming, and UV radiation on phytoplankton, *J. Appl.*  
723 *Phycol.*, 30, 743-759, [https://doi.org/ 10.1007/s10811-017-1329-6](https://doi.org/10.1007/s10811-017-1329-6), 2018.
- 724 Gerecht, A. C., Šupraha, L., Edvardsen, B., Probert, I., and Henderiks, J.: High  
725 temperature decreases the PIC/POC ratio and increases phosphorus requirements  
726 in *Coccolithus pelagicus* (Haptophyta), *Biogeosciences*, 11, 3531-3545,  
727 [https://doi.org/ 10.5194/bg-11-3531-2014](https://doi.org/10.5194/bg-11-3531-2014), 2014.
- 728 Gobler, C. J., Doherty, O. M., Hattenrath-Lehmann, T. K., Griffith, A. W., Kang, Y., and  
729 Litaker, R. W.: Ocean warming since 1982 has expanded the niche of toxic algal  
730 blooms in the North Atlantic and North Pacific oceans, *Proceedings of the*  
731 *National Academy of Sciences*, 201619575, [https://doi.org/](https://doi.org/10.1073/pnas.1619575114)  
732 [10.1073/pnas.1619575114](https://doi.org/10.1073/pnas.1619575114), 2017.
- 733 Hallegraeff, G. M.: Ocean climate change, phytoplankton community responses, and  
734 harmful algal blooms: a formidable predictive challenge, *J. Phycol.*, 46, 220-235,  
735 [https://doi.org/ 10.1111/j.1529-8817.2010.00815.x](https://doi.org/10.1111/j.1529-8817.2010.00815.x), 2010.
- 736 Hare, C. E., Leblanc, K., Ditullio, G. R., Kudela, R. M., Zhang, Y., Lee, P. A., Riseman,  
737 S., and Hutchins, D. A.: Consequences of increased temperature and CO<sub>2</sub> for  
738 phytoplankton community structure in the Bering Sea, *Marine Ecology Progress*,  
739 352, 9-16, [https://doi.org/ 10.3354/meps07182](https://doi.org/10.3354/meps07182), 2007.



- 740 Holligan, P., Viollier, M., Harbour, D., Camus, P., and Champagne-Philippe, M.:  
741 Satellite and ship studies of coccolithophore production along a continental shelf  
742 edge, *Nature*, 304, 339, <https://doi.org/10.1038/304339a0>, 1983.
- 743 Holligan, P. M., Fernández, E., Aiken, J., Balch, W. M., Boyd, P., Burkill, P. H., Finch,  
744 M., Groom, S. B., Malin, G., and Muller, K.: A biogeochemical study of the  
745 coccolithophore, *Emiliana huxleyi*, in the North Atlantic, *Global Biogeochem.*  
746 *Cycles*, 7, 879-900, <https://doi.org/10.1029/93GB01731>, 1993.
- 747 Hoppe, C., Langer, G., and Rost, B.: *Emiliana huxleyi* shows identical responses to  
748 elevated pCO<sub>2</sub> in TA and DIC manipulations, *J. Exp. Mar. Bio. Ecol.*, 406, 54-62,  
749 <https://doi.org/10.1016/j.jembe.2011.06.008>, 2011.
- 750 Hutchins, D. A., and Fu, F.: Microorganisms and ocean global change, *Nat Microbiol*,  
751 2, 17058, <https://doi.org/10.1038/nmicrobiol.2017.58>, 2017.
- 752 Iglesias-Rodríguez, M. D., Brown, C. W., Doney, S. C., Kleypas, J., Kolber, D., Kolber,  
753 Z., Hayes, P. K., and Falkowski, P. G.: Representing key phytoplankton functional  
754 groups in ocean carbon cycle models: Coccolithophorids, *Global Biogeochem.*  
755 *Cycles*, 16, 47-41-47-20, <https://doi.org/10.1029/2001GB001454>, 2002.
- 756 Jiang, L., Sun, Y.-F., Zhang, Y.-Y., Zhou, G.-W., Li, X.-B., McCook, L. J., Lian, J.-S.,  
757 Lei, X.-M., Liu, S., and Cai, L.: Impact of diurnal temperature fluctuations on  
758 larval settlement and growth of the reef coral *Pocillopora damicornis*,  
759 *Biogeosciences*, 14, 5741-5752, <https://doi.org/10.5194/bg-14-5741-2017>, 2017.
- 760 Keys, M., Tilstone, G., Findlay, H. S., Widdicombe, C. E., and Lawson, T.: Effects of  
761 elevated CO<sub>2</sub> and temperature on phytoplankton community biomass, species



762 composition and photosynthesis during an experimentally induced autumn bloom  
763 in the western English Channel, *Biogeosciences*, 15, 3203-3222, [https://doi.org/](https://doi.org/10.5194/bg-15-3203-2018)  
764 10.5194/bg-15-3203-2018, 2018.

765 Klaas, C., and Archer, D. E.: Association of sinking organic matter with various types  
766 of mineral ballast in the deep sea: Implications for the rain ratio, *Global*  
767 *Biogeochem. Cycles*, 16, 63-61-63-14, [https://doi.org/ 10.1029/2001GB001765](https://doi.org/10.1029/2001GB001765),  
768 2002.

769 Kremer, C. T., Fey, S. B., Arellano, A. A., and Vasseur, D. A.: Gradual plasticity alters  
770 population dynamics in variable environments: thermal acclimation in the green  
771 alga *Chlamydomonas reinhardtii*, *Proceedings Biological Sciences*, 285,  
772 20171942, [https://doi.org/ 10.1098/rspb.2017.1942](https://doi.org/10.1098/rspb.2017.1942), 2018.

773 Krumhardt, K. M., Lovenduski, N. S., Iglesias-Rodriguez, M. D., and Kleypas, J. A.:  
774 Coccolithophore growth and calcification in a changing ocean, *Prog. Oceanogr.*,  
775 159, 276-295, [https://doi.org/ 10.1016/j.pocean.2017.10.007](https://doi.org/10.1016/j.pocean.2017.10.007), 2017.

776 Matson, P. G., Ladd, T. M., Halewood, E. R., Sangodkar, R. P., Chmelka, B. F., and  
777 Iglesias-Rodriguez, M. D.: Intraspecific differences in biogeochemical responses  
778 to thermal change in the coccolithophore *Emiliana huxleyi*, *PLoS One*, 11,  
779 e0162313, <https://doi.org/10.1371/journal.pone.0162313>, 2016.

780 Monteiro, F. M., Bach, L. T., Brownlee, C., Bown, P., Rickaby, R. E., Poulton, A. J.,  
781 Tyrrell, T., Beaufort, L., Dutkiewicz, S., and Gibbs, S.: Why marine phytoplankton  
782 calcify, *Science Advances*, 2, e1501822, [https://doi.org/ 10.1126/sciadv.1501822](https://doi.org/10.1126/sciadv.1501822),  
783 2016.



- 784 Morán, X. A. G., LÓPEZ-URRUTIA, Á., CALVO-DÍAZ, A., and Li, W. K.: Increasing  
785 importance of small phytoplankton in a warmer ocean, *Glob. Chang. Biol.*, 16,  
786 1137-1144, <https://doi.org/10.1111/j.1365-2486.2009.01960.x>, 2010.
- 787 Neukermans, G., Oziel, L., and Babin, M.: Increased intrusion of warming Atlantic  
788 water leads to rapid expansion of temperate phytoplankton in the Arctic, *Glob.*  
789 *Chang. Biol.*, <https://doi.org/10.1111/gcb.14075>, 2018.
- 790 Norberg, J.: Biodiversity and ecosystem functioning: a complex adaptive systems  
791 approach, *Limnol. Oceanogr.*, 49, 1269-1277, [https://doi.org/](https://doi.org/10.4319/lo.2004.49.4_part_2.1269)  
792 [10.4319/lo.2004.49.4\\_part\\_2.1269](https://doi.org/10.4319/lo.2004.49.4_part_2.1269), 2004.
- 793 O'Donnell, D. R., Hamman, C. R., Johnson, E. C., Kremer, C. T., Klausmeier, C. A.,  
794 and Litchman, E.: Rapid thermal adaptation in a marine diatom reveals constraints  
795 and tradeoffs, *Glob. Chang. Biol.*, doi:10.1111/gcb.14360, 2018.
- 796 Oliver, T., and Palumbi, S.: Do fluctuating temperature environments elevate coral  
797 thermal tolerance?, *Coral Reefs*, 30, 429-440, [https://doi.org/10.1007/s00338-](https://doi.org/10.1007/s00338-011-0721-y)  
798 [011-0721-y](https://doi.org/10.1007/s00338-011-0721-y), 2011.
- 799 Paasche, E.: Reduced coccolith calcite production under light-limited growth: a  
800 comparative study of three clones of *Emiliana huxleyi* (Prymnesiophyceae),  
801 *Phycologia*, 38, 508-516, 1999.
- 802 Paasche, E.: A review of the coccolithophorid *Emiliana huxleyi* (Prymnesiophyceae),  
803 with particular reference to growth, coccolith formation, and calcification-  
804 photosynthesis interactions, *Phycologia*, 40, 503-529, [https://doi.org/](https://doi.org/10.2216/i0031-8884-40-6-503.1)  
805 [10.2216/i0031-8884-40-6-503.1](https://doi.org/10.2216/i0031-8884-40-6-503.1), 2001.



- 806 Rasconi, S., Winter, K., and Kainz, M. J.: Temperature increase and fluctuation induce  
807 phytoplankton biodiversity loss—Evidence from a multi-seasonal mesocosm  
808 experiment, *Ecology and evolution*, 7, 2936-2946, [https://doi.org/](https://doi.org/10.1002/ece3.2889)  
809 10.1002/ece3.2889, 2017.
- 810 Raven, J. A., and Crawford, K.: Environmental controls on coccolithophore  
811 calcification, *Mar. Ecol. Prog. Ser.*, 470, 137-166, [https://doi.org/](https://doi.org/10.3354/meps09993)  
812 10.3354/meps09993, 2012.
- 813 Riegman, R., Stolte, W., Noordeloos, A. A., and Slezak, D.: Nutrient uptake and  
814 alkaline phosphatase (EC 3: 1: 3: 1) activity of *Emiliana huxleyi*  
815 (Prymnesiophyceae) during growth under N and P limitation in continuous  
816 cultures, *J. Phycol.*, 36, 87-96, [https://doi.org/ 10.1046/j.1529-8817.2000.99023.x](https://doi.org/10.1046/j.1529-8817.2000.99023.x),  
817 2000.
- 818 Rosas-Navarro, A., Langer, G., and Ziveri, P.: Temperature affects the morphology and  
819 calcification of *Emiliana huxleyi* strains, *Biogeosciences*, 13, 2913-2926,  
820 <https://doi.org/10.5194/bg-13-2913-2016>, 2016.
- 821 Safaie, A., Silbiger, N. J., McClanahan, T. R., Pawlak, G., Barshis, D. J., Hench, J. L.,  
822 Rogers, J. S., Williams, G. J., and Davis, K. A.: High frequency temperature  
823 variability reduces the risk of coral bleaching, *Nat Commun*, 9, [https://doi.org/](https://doi.org/10.1038/s41467-018-04074-2)  
824 10.1038/s41467-018-04074-2, 2018.
- 825 Schaum, C. E., and Collins, S.: Plasticity predicts evolution in a marine alga,  
826 *Proceedings of the Royal Society B: Biological Sciences*, 281, 20141486,  
827 [https://doi.org/ 10.1098/rspb.2014.1486](https://doi.org/10.1098/rspb.2014.1486), 2014.



- 828 Schaum, C. E., Buckling, A., Smirnov, N., Studholme, D., and Yvondurocher, G.:  
829 Environmental fluctuations accelerate molecular evolution of thermal tolerance in  
830 a marine diatom, *Nat Commun*, 9, 1719, [https://doi.org/ 10.1038/s41467-018-](https://doi.org/10.1038/s41467-018-03906-5)  
831 [03906-5](https://doi.org/10.1038/s41467-018-03906-5), 2018.
- 832 Schaum, E., Rost, B., Millar, A. J., and Collins, S.: Variation in plastic responses of a  
833 globally distributed picoplankton species to ocean acidification, *Nature Climate*  
834 *Change*, 3, 298-302, [https://doi.org/ 10.1038/NCLIMATE1774](https://doi.org/10.1038/NCLIMATE1774), 2013.
- 835 Schlüter, L., Kai, T. L., Gutowska, M. A., Gröger, J. P., Riebesell, U., and Reusch, T. B.  
836 H.: Adaptation of a globally important coccolithophore to ocean warming and  
837 acidification, *Nature Climate Change*, 4, 1024-1030, [https://doi.org/](https://doi.org/10.1038/nclimate2379)  
838 [10.1038/nclimate2379](https://doi.org/10.1038/nclimate2379), 2014.
- 839 Sett, S., Bach, L. T., Schulz, K. G., Koch-Klavsen, S., Lebrato, M., and Riebesell, U.:  
840 Temperature modulates coccolithophorid sensitivity of growth, photosynthesis  
841 and calcification to increasing seawater pCO<sub>2</sub>, *PLoS One*, 9, e88308,  
842 [https://doi.org/ 10.1371/journal.pone.0088308](https://doi.org/10.1371/journal.pone.0088308), 2014.
- 843 Shurin, J. B., Winder, M., Adrian, R., Keller, W., Matthews, B., Paterson, A. M.,  
844 Paterson, M. J., Pinel-Alloul, B., Rusak, J. A., and Yan, N. D.: Environmental  
845 stability and lake zooplankton diversity—contrasting effects of chemical and  
846 thermal variability, *Ecol. Lett.*, 13, 453-463, [https://doi.org/ 10.1111/j.1461-](https://doi.org/10.1111/j.1461-0248.2009.01438.x)  
847 [0248.2009.01438.x](https://doi.org/10.1111/j.1461-0248.2009.01438.x), 2010.
- 848 Sunda, W. G., Price, N. M., and Morel, F. M.: Trace metal ion buffers and their use in  
849 culture studies, *Algal culturing techniques*, 4, 35-63, 2005.



- 850 Sunday, J. M., Bates, A. E., and Dulvy, N. K.: Thermal tolerance and the global  
851 redistribution of animals, *Nature Climate Change*, 2, 686, [https://doi.org/](https://doi.org/10.1038/nclimate1539)  
852 10.1038/nclimate1539, 2012.
- 853 Tatters, A. O., Schnetzer, A., Xu, K., Walworth, N. G., Fu, F., Spackeen, J. L., Sipler,  
854 R. E., Bertrand, E. M., McQuaid, J. B., and Allen, A. E.: Interactive effects of  
855 temperature, CO<sub>2</sub> and nitrogen source on a coastal California diatom assemblage,  
856 *J. Plankton Res.*, 40, 151-164, 2018.
- 857 Thomas, M. K., Kremer, C. T., Klausmeier, C. A., and Litchman, E.: A global pattern  
858 of thermal adaptation in marine phytoplankton, *Science*, 338, 1085-1088,  
859 [https://doi.org/ 10.1126/science.1224836](https://doi.org/10.1126/science.1224836), 2012.
- 860 Vázquez, D. P., Gianoli, E., Morris, W. F., and Bozinovic, F.: Ecological and  
861 evolutionary impacts of changing climatic variability, *Biological Reviews*, 92, 22-  
862 42, [https://doi.org/ 10.1111/brv.12216](https://doi.org/10.1111/brv.12216), 2017.
- 863 Vasseur, D. A., DeLong, J. P., Gilbert, B., Greig, H. S., Harley, C. D., McCann, K. S.,  
864 Savage, V., Tunney, T. D., and O'Connor, M. I.: Increased temperature variation  
865 poses a greater risk to species than climate warming, *Proceedings of the Royal*  
866 *Society of London B: Biological Sciences*, 281, 20132612, [https://doi.org/](https://doi.org/10.1098/rspb.2013.2612)  
867 10.1098/rspb.2013.2612, 2014.
- 868 Westbroek, P., Brown, C. W., van Bleijswijk, J., Brownlee, C., Brummer, G. J., Conte,  
869 M., Egge, J., Fernández, E., Jordan, R., and Knappertsbusch, M.: A model system  
870 approach to biological climate forcing. The example of *Emiliana huxleyi*, *Global*  
871 *Planet. Change*, 8, 27-46, 1993.



872 Yvon-Durocher, G., Allen, A. P., Cellamare, M., Dossena, M., Gaston, K. J., Leitaó, M.,  
873 Montoya, J. M., Reuman, D. C., Woodward, G., and Trimmer, M.: Five years of  
874 experimental warming increases the biodiversity and productivity of  
875 phytoplankton, PLoS Biol., 13, e1002324, [https://doi.org/](https://doi.org/10.1371/journal.pbio.1002324)  
876 10.1371/journal.pbio.10023242015.

877 Zander, A., Bersier, L. F., and Gray, S. M.: Effects of temperature variability on  
878 community structure in a natural microbial food web, Glob. Chang. Biol., 23, 56-  
879 67, <https://doi.org/10.1111/gcb.13374>, 2017.

880 Zhang, M., Qin, B., Yu, Y., Yang, Z., Shi, X., and Kong, F.: Effects of temperature  
881 fluctuation on the development of cyanobacterial dominance in spring:  
882 Implication of future climate change, Hydrobiologia, 763, 135-146,  
883 <https://doi.org/10.1007/s10750-015-2368-0>, 2016.

884 Zhu, Z., Qu, P., Fu, F., Tennenbaum, N., Tatters, A. O., and Hutchins, D. A.:  
885 Understanding the blob bloom: Warming increases toxicity and abundance of the  
886 harmful bloom diatom *Pseudo-nitzschia* in California coastal waters, Harmful  
887 Algae, 67, 36-43, <https://doi.org/10.1016/j.hal.2017.06.004>, 2017.

888  
889  
890



891 **Figure legends:**

892 **Fig. 1** Thermal performance curves (TPCs) showing cell-specific growth rates ( $d^{-1}$ ) of  
893 *Emiliana huxleyi* CCMP371 across a temperature range from 8.5 to 28.6 °C. Symbols  
894 represent means and error bars are the standard deviations of three replicates at each  
895 temperature, but in many cases the errors bars are smaller than the symbols.

896 **Fig. 2** Changes in *Emiliana huxleyi* TPC/PON ratios, POC/PON ratios, PIC/POC ratios  
897 and Cha/POC ratios across a temperatures range from 8.5 to 28.6 °C. Dashed lines  
898 represent the average ratios for the entire temperature range. Bars represent means and  
899 error bars are the standard deviations of three replicates at each temperature. Symbols  
900 \* represent the significant difference ( $p < 0.05$ ) between average ratios and the ratio at  
901 each temperature.

902 **Fig. 3** *Emiliana huxleyi* growth rate responses to constant temperatures, and during the  
903 warm and cool phases of the two thermal variation frequencies (one-day and two-day),  
904 under low (**A**) and high (**B**) mean temperatures. The thick black line in the boxplots  
905 represent median values for each experimental treatment; whiskers on boxplots indicate  
906  $1.5 \times$  interquartile range. Listed p-values with their respective brackets are the statistical  
907 significance between two treatments.

908 **Fig. 4** Responses of *Emiliana huxleyi* PIC/POC ratios to constant temperatures, and  
909 during the warm and cool phases of two thermal variation frequencies (one-day and  
910 two-day), under low (**A**) and high (**B**) mean temperatures. LT: Low temperature; HT:  
911 High temperature. The thick black line in the boxplots represent median values for each  
912 experimental treatment; whiskers on boxplots indicate  $1.5 \times$  interquartile range. Listed



913 p-values with their respective brackets denote the statistical significance between two  
914 treatments.

915 **Fig. 5** Responses of *Emiliana huxleyi* total carbon fixation (photosynthesis +  
916 calcification), photosynthetic and calcification rates to constant temperatures, and  
917 during the warm and cool phases of two thermal variation frequencies (one-day and  
918 two-day), under low (**A, C, E**) and high (**B, D, F**) mean temperatures. LT: Low  
919 temperature; HT: High temperature. The thick black line in the boxplots represent  
920 median values for each experimental treatment; whiskers on boxplots indicate  $1.5 \times$   
921 interquartile range. Listed p-values with their respective brackets denote the statistical  
922 significance between two treatments.

923 **Fig. 6** Responses of *Emiliana huxleyi* calcification to photosynthesis ratios (cal/photo)  
924 to constant temperatures, and during the warm and cool phases of two thermal variation  
925 frequencies (1 day and 2 day), under low (**A**) and high (**B**) mean temperatures. LT: Low  
926 temperature; HT: High temperature. The thick black line in the boxplots represent  
927 median values for each experimental treatment; whiskers on boxplots indicate  $1.5 \times$   
928 interquartile range. Listed p-values with their respective brackets denote the statistical  
929 significance between two treatments.

930 **Fig. 7** Responses of *Emiliana huxleyi* elemental ratios in two thermal variation  
931 frequency treatments (1 day and 2 day) compared to constant temperatures, for:  
932 TPC/PON (**A**, cool phase and **B**, warm phase), PON/POP (**C**, cool phase and **D**, warm  
933 phase) and Chl *a*/POC ratios (**E**, cool phase and **F**, warm phase). LT: Low temperature;  
934 HT: High temperature. The thick black line in the boxplots represent median values for



935 each experimental treatment; whiskers on boxplots indicate  $1.5 \times$  interquartile range.  
936 Listed p-values with their respective brackets denote the statistical significance between  
937 two treatments.

938 **Fig. 8** Thermal performance curves (TPCs) based on specific growth rates ( $d^{-1}$ ) of  
939 *Emiliana huxleyi*, including our experimentally determined constant temperature TPC  
940 (black symbols and solid line) and an Eppley model-predicted fluctuating temperature  
941 TPC (dashed line). Measured growth rates from the two low and high temperature  
942 experiments are shown for constant thermal conditions (red symbols), one-day (green  
943 symbols) and two-day (blue symbols) variation treatments.

944



945 Table 1 The effect of temperature variation under low and high temperature on total Carbon (pg/cell), cellular POC (pg/cell), cellular PIC (pg/cell), cellular PON (pg/cell), cellular POP (pg/cell) and cellular Chl *a* (pg/cell) of *Emiliania huxleyi*.  
 946

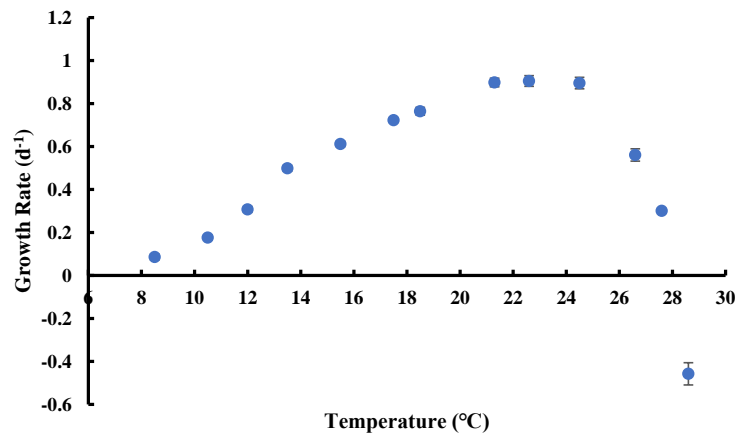
Treatment	Total Carbon	Cellular PON	Cellular POP	Cellular POC	Cellular PIC	Cellular Chl <i>a</i>	
<b>low temperature</b>	18.5 °C	11.5±0.4	1.8±0.2	0.17±0.00	8.0±0.6	3.5±0.3	0.14±0.00
	One-day cool point (16)	13.0±0.5	2.2±0.3	0.18±0.00	8.9±0.3	4.1±0.3	0.15±0.01
	One-day warm point (21)	12.0±0.7	2.1±0.3	0.19±0.00	9.3±0.9	2.7±0.9	0.19±0.00
	Two-day cool point (16)	10.1±0.7	1.3±0.2	0.16±0.01	6.0±0.9	4.0±0.3	0.12±0.01
	Two-day warm point (21)	10.4±0.5	1.5±0.2	0.17±0.01	6.6±0.5	3.8±0.3	0.15±0.01
<b>high temperature</b>	25.5 °C	15.0±0.7	2.0±0.1	0.21±0.01	9.5±0.3	5.5±0.7	0.18±0.02
	One-day cool point (23)	16.1±1.4	3.0±0.2	0.21±0.00	12.9±1.5	3.2±0.2	0.15±0.01
	One-day warm point (28)	19.1±0.8	4.4±0.3	0.24±0.01	17.0±0.6	2.1±0.2	0.20±0.02
	Two-day cool point (23)	12.4±1.0	1.9±0.2	0.19±0.01	7.5±1.0	4.8±0.3	0.13±0.01
	Two-day warm point (28)	19.4±2.0	3.9±0.8	0.25±0.03	18.3±3.7	2.1±0.9	0.25±0.02

947

948



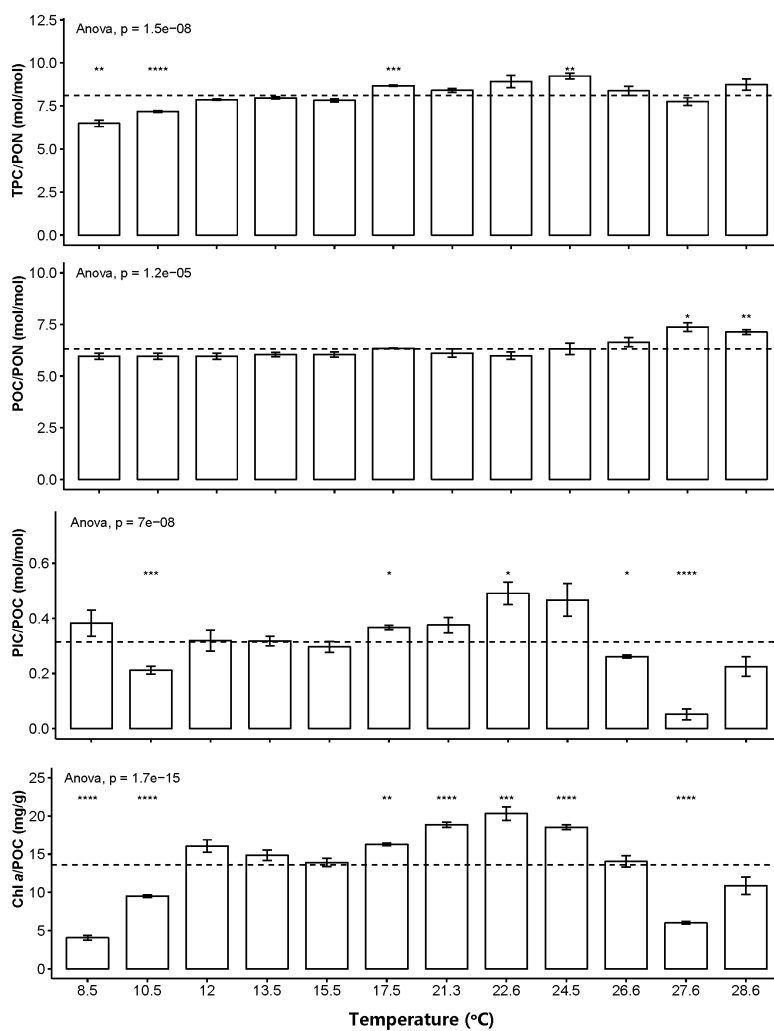
949 Fig. 1



950



951 **Fig. 2**

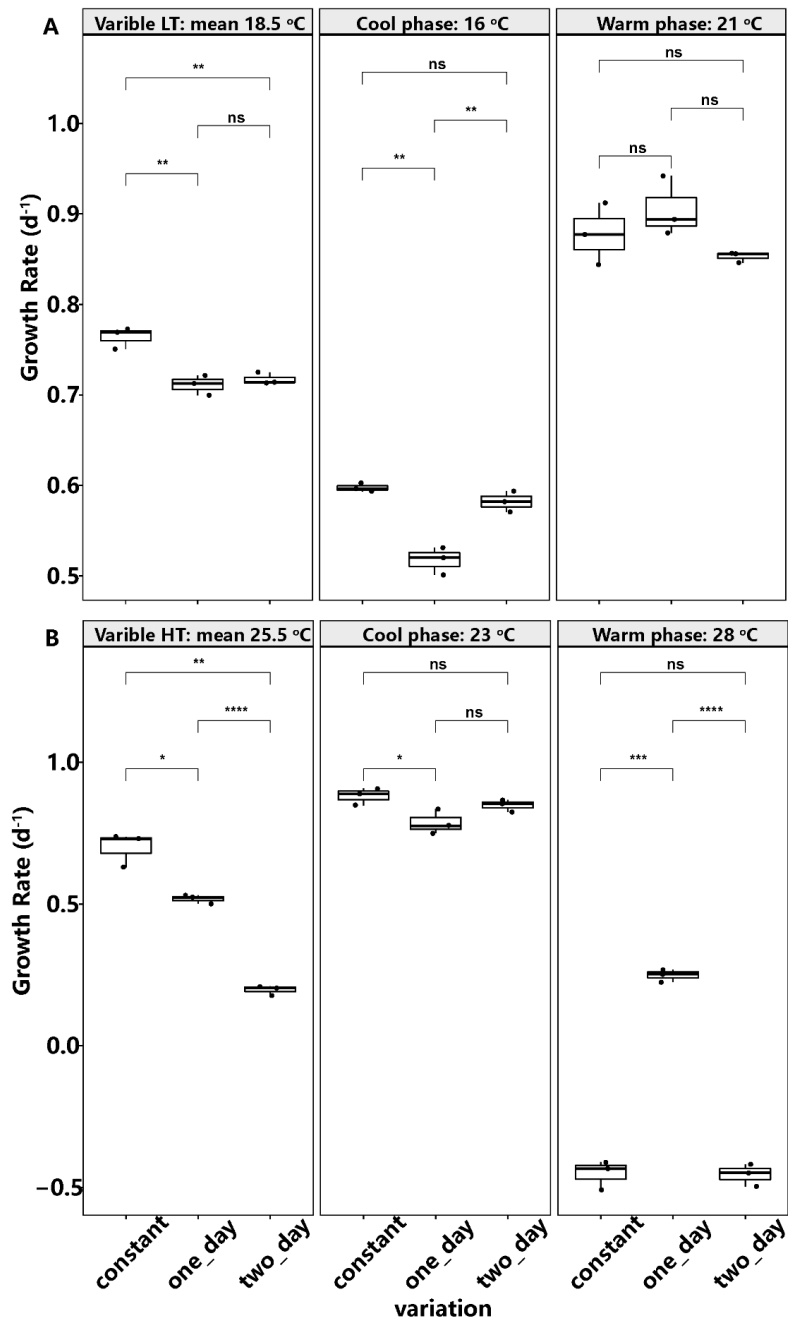


952

953

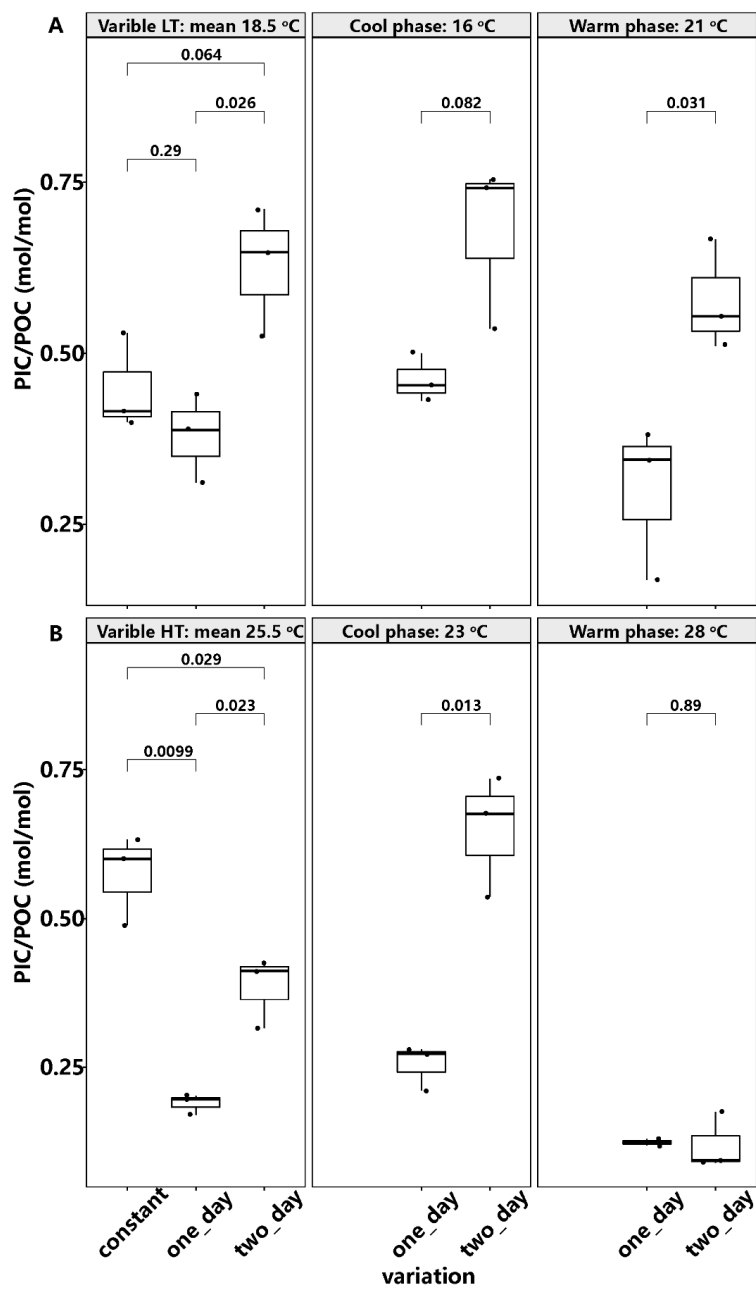


954 Fig. 3





956 Fig. 4



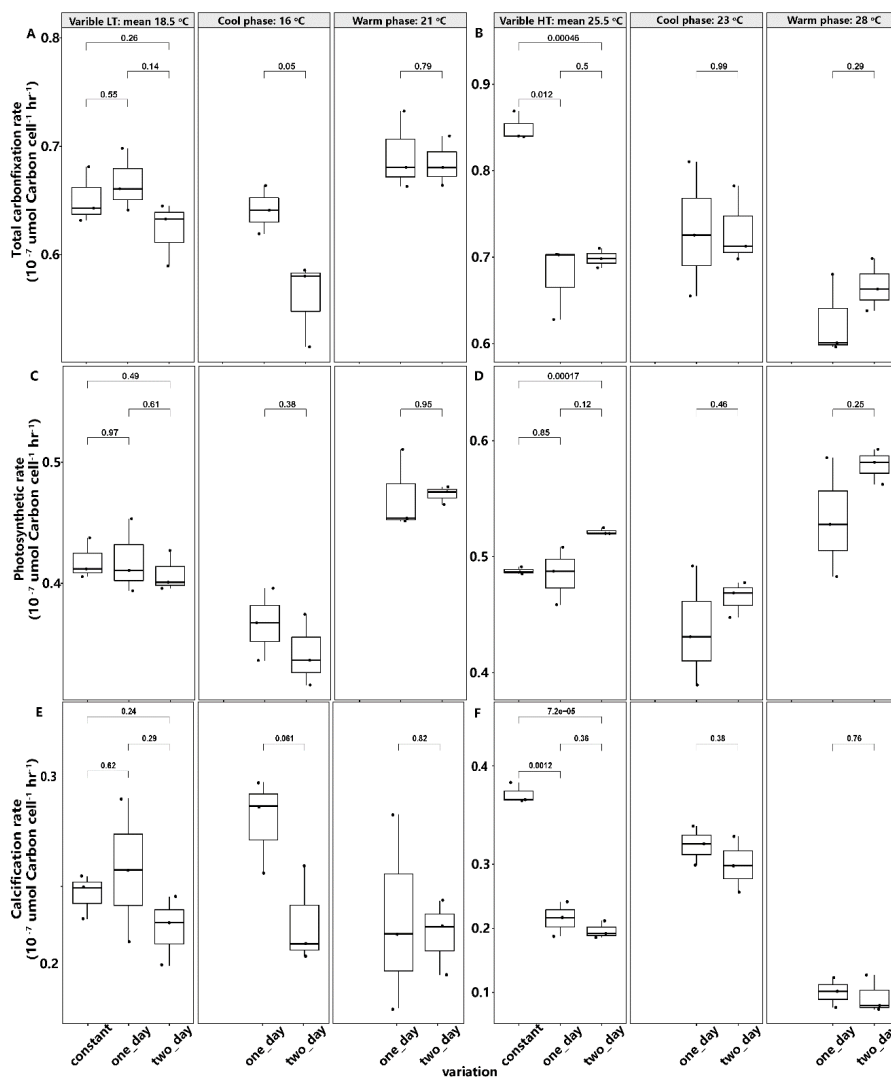
957

958



959 **Fig. 5**

960

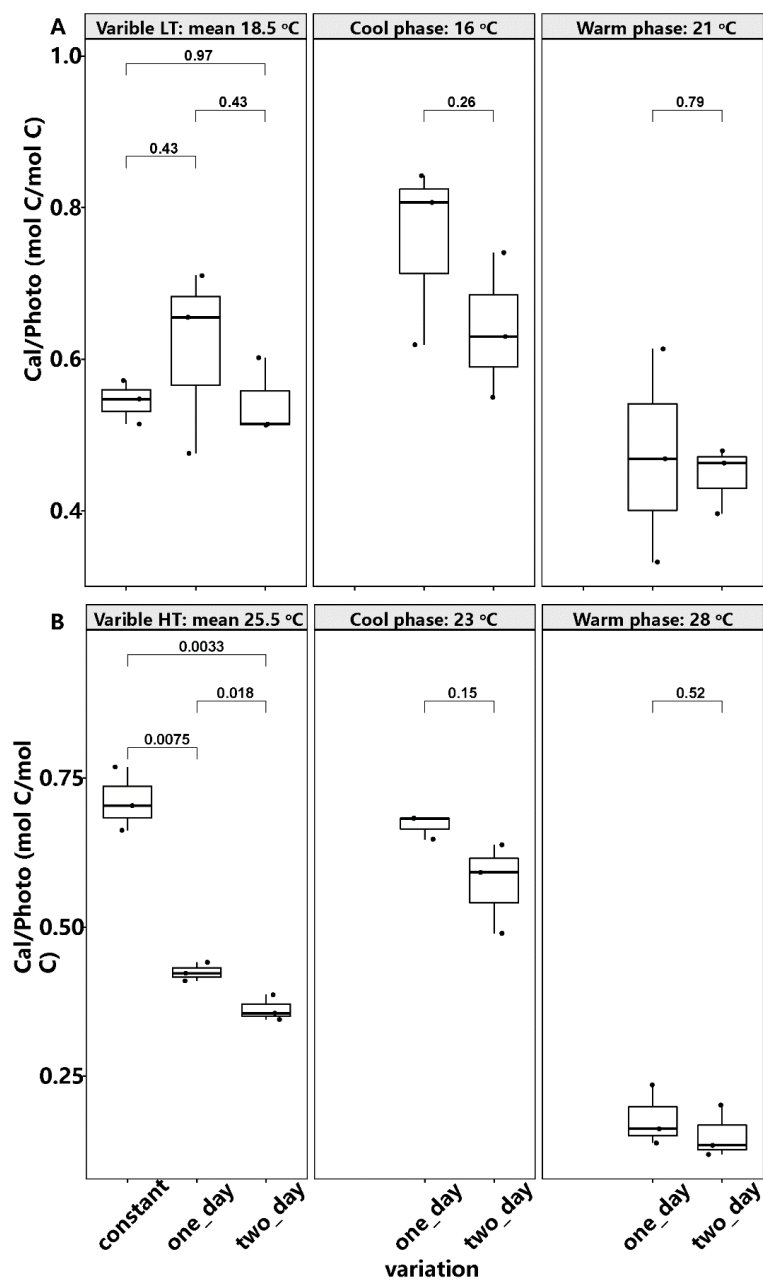


961

962



963 Fig. 6

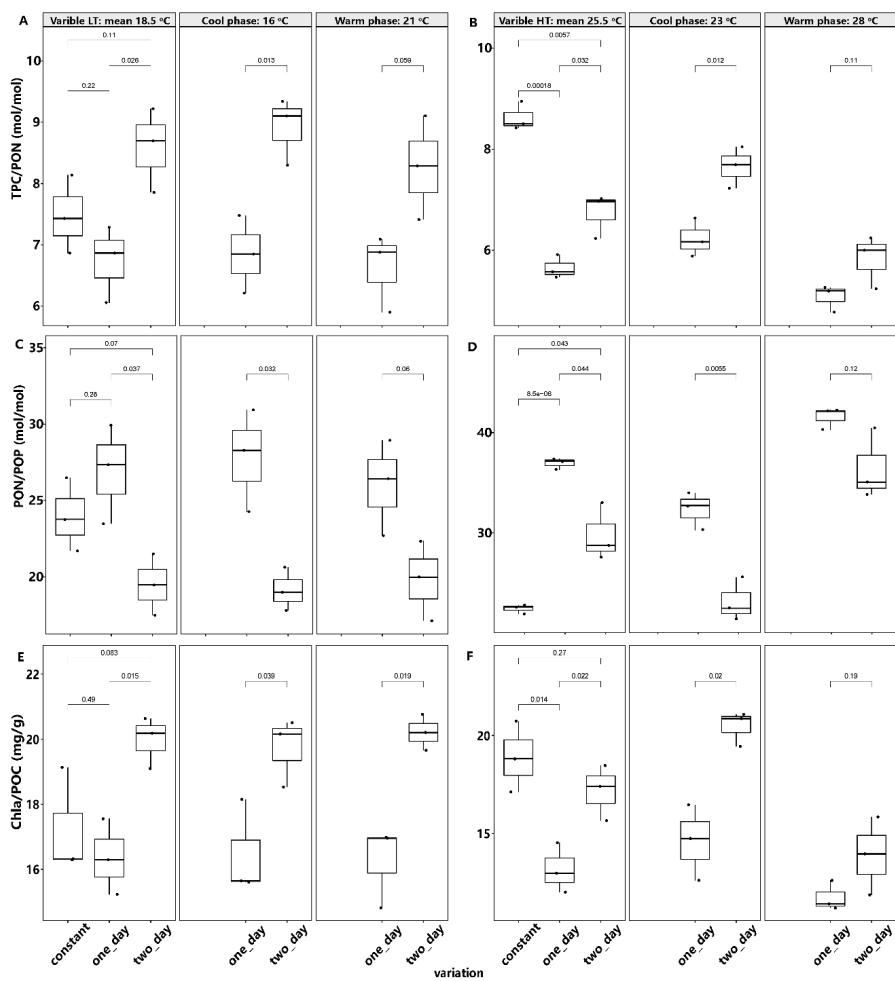


964

965



966 **Fig. 7**

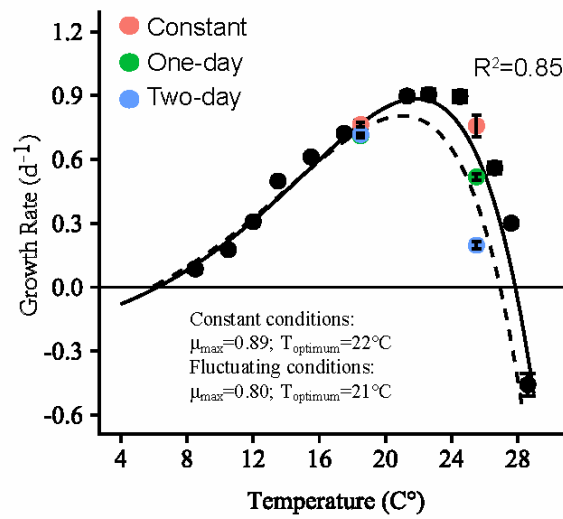


967

968



969 Fig. 8



970